

Scattering-induced entanglement between spin qubits at remote two-state structures

This article has been downloaded from IOPscience. Please scroll down to see the full text article.

2009 J. Phys.: Condens. Matter 21 075503

(<http://iopscience.iop.org/0953-8984/21/7/075503>)

View [the table of contents for this issue](#), or go to the [journal homepage](#) for more

Download details:

IP Address: 129.252.86.83

The article was downloaded on 29/05/2010 at 17:52

Please note that [terms and conditions apply](#).

Scattering-induced entanglement between spin qubits at remote two-state structures

Matthew Habgood¹, John H Jefferson^{1,2} and G Andrew D Briggs¹

¹ QIP IRC Group, Department of Materials, University of Oxford, Parks Road, Oxford, UK

² QinetiQ, Sensors and Electronics Division, St Andrew's Road, Great Malvern, UK

Received 4 October 2008, in final form 8 January 2009

Published 29 January 2009

Online at stacks.iop.org/JPhysCM/21/075503

Abstract

A theoretical scheme is presented for the entanglement of two-electron spin qubits bound in series within a quasi-one-dimensional mesoscopic structure at a distance beyond their normal range of interaction. A third electron is scattered from them, and full entanglement is achieved upon measurement of a transmitted electron in the correct spin state. Critically, each bound electron is trapped within an individual structure that has at least two spatial states. Two simple examples of such structures are discussed here. One is a 'stub', in which a quantum dot (for example) is coupled to one side of the quasi-one-dimensional structure. The other is a pair of degenerate, coupled quantum dots, with strong interdot Coulomb repulsion, placed within the one-dimensional superstructure. Both of these are shown to allow generation of entanglement with a significant probability of success. In contrast to the results of the authors' previous works, this allows for the generation of entanglement in a series, rather than in a parallel, configuration of the bound electrons with respect to the propagating electron.

1. Introduction

Experimental technologies for the realization of qubits as electron spins in the solid state are rapidly progressing at the present time. A prominent example of these technologies is the use of quantum dots (QDs) to isolate and control individual electron spin qubits [1–5]. These systems offer relatively long coherence and spin relaxation times along with exploitation of existing solid state technologies. The majority of the existing work in this field has used gate-defined QDs in semiconductor environments, but it has also been recognized that mesoscopic molecular carbon environments, such as [6, 7] fullerenes and carbon nanotubes, have potential as qubit hosts, including increased coherence and relaxation times, in addition to the possibility of limited ballistic and coherent electron transport in the nanotubes [8, 9, 7, 6]. The use of carbon nanotubes, which are pseudo-one-dimensional structures, enables spin qubits to be ordered and addressed in a controlled manner, at pseudo-zero-dimensional structures along the length of a tube. Recent research in this area has focused on the use of gate-defined QDs [10–12].

In the context of a one-dimensional array of bound spin qubits, a 'flying qubit' could be used to mediate interactions between the constituent qubits. A flying qubit is a mobile physical system which also acts as a qubit in itself. An obvious candidate for such a system in the solid state is

another electron, this time able to propagate rather than being bound at a QD—an electron traveling along a carbon nanotube, for example. Such a flying qubit could induce entanglement between two 'static' qubits well beyond the range of their direct interactions, for example by scattering from them in a spin-dependent manner. In order to explore this possibility theoretically, a quantum dot embedded in a one-dimensional structure can be modeled using a 'real-space Anderson' Hamiltonian [13]. This Hamiltonian represents the quantum dot as a single binding site in a discretized chain, with a distinct on-site single-electron energy and a Coulomb repulsion. It is labeled 'real-space Anderson' in reference to the original Anderson model [14], which models magnetic impurities in metals as a single energy level with a Coulomb repulsion coupled to a continuum of states.

Using this [13] and other [15, 16] methods, it has been demonstrated that a propagating electron can be fully entangled with a bound electron by scattering. For the appropriate propagation momenta, a combination of strong backscattering and Coulomb-mediated resonance achieves near-complete separation of the singlet and triplet states with respect to transmission and reflection. Unfortunately, as the authors of this study have reported elsewhere [17] this means that the scattering of a propagating electron cannot entangle the spins of two electrons bound at real-space Anderson sites in series, with any significant probability of success. This is one example of the monogamy theorem [18].

In this study, it is shown that a modest addition to the real-space Anderson binding structure—the expansion of the one-spatial-state binding structure to include two spatial states—will allow the spins of two electrons bound in series to be entangled with a reasonably high probability of success (up to ~ 0.24). These structures that give rise to two single-electron spatial states, referred to for brevity as ‘two-state structures’, are represented in a modification of the real-space Anderson model. Each bound electron is placed at a separate two-state binding structure (see figure 1). Although the authors have reported elsewhere [17] on the possible generation of entanglement between bound electrons in a parallel configuration, the approach described here allows for a (experimentally much simpler) series configuration. It also represents a new approach to the entanglement-by-scattering problem, actively exploiting the additional degree of freedom available to the qubit-bearing electrons (the additional spatial state) to enhance the degree of entanglement.

A few previous theoretical studies [19–23] have predicted the entanglement of static spins in series by scattering of a propagating electron. These studies have modeled the interaction between the propagating and the static spins using an exchange-type interaction that is ‘switched on’ when the propagating electron occupies a specified point in space, the point of closest approach to the static spin. In reference to its resemblance to the *s*–*d* model [14], in which electrons in a continuum interact with a fixed, external spin via an exchange-type coupling, this is labeled for convenience as the ‘point *s*–*d*’ model in this study. This will be discussed further in section 2.

The idea of using a mobile mediating agent to create entanglement between two qubits beyond the effective range of interaction between their physical embodiments is even older [24]; the concept was first applied to electron spins in the solid state by Leuenberger *et al* [25], with the proposed use of a photon as a mediating agent. Although photons have greater coherence lengths than electrons, the investigation of propagating electrons as mediating agents continues in this study (among others). The reason for this is simply that bringing about useful interactions between photons and electrons requires a radically different experimental set-up to that used for electron waveguides and/or nanowires (compare the techniques of [26], in which spin operations are carried out with photons, to those of [12], a candidate system for development into the scheme proposed in this study). At this comparatively early stage in the development of solid state quantum computing, it is difficult to say which of the two kinds of electron spin-based system will be most useful. The superior coherence characteristics of the photon will only be one factor in making this decision. At the current time, it is therefore desirable to continue the theoretical investigation of both electronic and photonic approaches to the use of a mediating agent.

The use of two-state Anderson-type binding structures for the bound electrons means that backscattering and Coulomb-mediated resonance will not automatically result in high singlet/triplet filtering, and hence entanglement can in principle be produced by scattering between two electrons bound in series. An additional requirement on a system

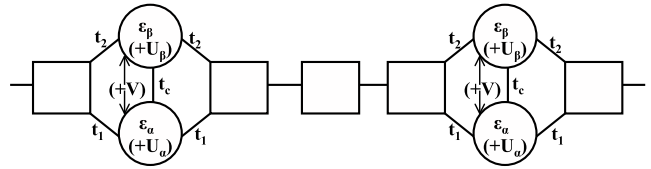


Figure 1. Two general two-state binding structures in the real-space Anderson model. See section 2, equations (1)–(4) and accompanying discussion for more details.

corresponding to the Anderson-type model in this scheme is that neither of the bound electrons should be ionized. Considering this requirement, this study focuses on two simple examples of two-state binding structures. In the first, a single-state binding site is placed to one side of a one-dimensional structure, and couples to one discretized site in that structure (the latter is the spatially-defined ‘second state’ of the binding structure, in this case). In the second, one state of the binding structure is embedded in the one-dimensional structure, and the second state (assumed to be near-degenerate) is coupled to the first.

The basic form of the individual structures is similar to that proposed by Loss and Sukhorukov [27] for the measurement of entanglement between two spins. In the current study, however, the electrons to be entangled are localized at separate two-state structures placed in series. This is in distinction to the work of Loss and Sukhorukov, in which the electrons occupy two states (quantum dots) of a single structure.

Using Anderson-type models for these two-state binding structures, this study calculates the spin-dependent scattering behavior of a propagating electron from two electrons bound in series at separate binding structures. In order to focus on the essentials of entanglement generation, all calculations are carried out in the elastic scattering regime, and the $S_z = \frac{1}{2}$ spin subspace. The behavior of the $S_z = -\frac{1}{2}$ subspace follows trivially by symmetry, and since no explicit spin-flip terms are included in the model, the $|S_z| = \frac{3}{2}$ subspaces are irrelevant to the generation of entanglement. The relevant three-electron spin states are therefore $|\downarrow\uparrow\uparrow\rangle$, $|\uparrow\downarrow\uparrow\rangle$ and $|\uparrow\uparrow\downarrow\rangle$. The degree of entanglement resulting from the scattering process will be dictated by the presence of the $|\downarrow\uparrow\rangle$ and $|\uparrow\downarrow\rangle$ states of the bound electrons after scattering, and hence by the spin-dependent scattering behavior. Scattering and entanglement calculations are reported for the ‘stub’ type two-state structure in section 3, and for the ‘double QD’ type structure in section 4. In both cases it is shown that careful tuning of the parameters can result in fully entangled bound electrons with a reasonable probability of success. Scattering and entanglement for the point *s*–*d* model are briefly revisited in section 2, in the context of the discretized model used for the one-dimensional structure in this study.

2. Theory and methodology

In this study, a quasi-one-dimensional structure containing two two-state binding structures is modeled as an ideal,

discretized chain of tight-binding-model-type sites, in which the states of the binding structures are treated as additional sites subject to differing on-site energies and two-electron Coulomb repulsions. The overall system is illustrated in figure 1.

The Hamiltonian for the system is

$$\hat{H} = \hat{H}_R + \hat{H}_L + \hat{H}_C + \hat{H}_I + \hat{H}_{BS}, \quad (1)$$

where

$$\hat{H}_R = - \left[\sum_{n=x_2+1}^{\infty} \sum_{\sigma} t c_{n+1\sigma}^{\dagger} c_{n\sigma} + \text{h.c.} \right] \quad (2)$$

is the Hamiltonian for the right lead. The Hamiltonian for the left lead, \hat{H}_L , is similar, with the summation over n running from $-\infty$ to $x_1 - 2$. The Hamiltonian for the structure intermediate between the binding structures, \hat{H}_C is also similar, with the summation over n running from $x_1 + 1$ to $x_2 - 2$. The leftmost and rightmost binding structures are located at x_1 and x_2 respectively. A single electron propagating in the ideal leads (or the intermediate structure) will occupy an energy band of the form $\varepsilon_k = -2t \cos k$.

The Hamiltonian for the binding structures is

$$\begin{aligned} \hat{H}_{BS} = & \sum_{n=x_1, x_2} \left(\sum_{m=\alpha, \beta} \sum_{\sigma} \varepsilon_m c_{n, m, \sigma}^{\dagger} c_{n, m, \sigma} \right. \\ & - \sum_{\sigma} (t_c c_{n, \alpha, \sigma}^{\dagger} c_{n, \beta, \sigma} + \text{h.c.}) + \sum_{m=\alpha, \beta} U_m n_{m\uparrow} n_{m\downarrow} \\ & \left. + \sum_{\sigma\sigma'} V n_{n\alpha\sigma} n_{n\beta\sigma'} \right). \quad (3) \end{aligned}$$

Here, $m = \alpha, \beta$ indexes the two states of each binding structure, which have corresponding single-electron energies of ε_m and intrastate Coulomb repulsions of U_m . The interstate Coulomb repulsion is V , while the interstate hopping parameter is t_c .

The Hamiltonian for the interaction of the leads (and the intermediate structure) with the binding structures is

$$\begin{aligned} \hat{H}_I = & - \sum_{n=x_1, x_2} \sum_{\sigma} [t_1 c_{n\alpha\sigma}^{\dagger} c_{n+1\sigma} + t_1 c_{n\alpha\sigma}^{\dagger} c_{n-1\sigma} + t_2 c_{n\beta\sigma}^{\dagger} c_{n+1\sigma} \\ & + t_2 c_{n\beta\sigma}^{\dagger} c_{n-1\sigma} + \text{h.c.}]. \quad (4) \end{aligned}$$

The coupling strengths are t_1 to state α and t_2 to state β . In the stub structure we have $\varepsilon_{\alpha} = U_{\alpha} = 0$, $\varepsilon_{\beta} = \varepsilon_0$, $U_{\beta} = U$, $V = 0$, $t_1 = t'$, $t_2 = 0$ and free choice of other parameters (in principle), to give a single-state binding site side-coupled to an otherwise ideal tight-binding structure. In the double QD structure, we have $\varepsilon_{\alpha} = \varepsilon_{\beta} = \varepsilon_0$, $U_{\alpha} = U_{\beta} = U$ and free choice of other parameters.

The objective of this study is to characterize the scattering behavior of a propagating electron in this system from two bound electrons, one bound at each binding structure. To calculate the necessary three-electron wavefunctions (all other electrons are included implicitly in the parameters of the Hamiltonian above) in a straightforward manner while capturing the scattering effects essential to the generation of entanglement, a few simplifying assumptions and approximations are made.

Firstly, the leads and the region between the binding structures are approximated as ideal periodic one-dimensional

structures, so a single-electron wavefunction for a propagating electron in those regions takes the form of a sum over left- and right-traveling plane waves multiplied by complex amplitudes, $A e^{ikn} + B e^{-ikn}$. Secondly, the binding structures are assumed to be tightly binding ($\varepsilon_0 \ll -t$), and sufficiently well separated that the spatial wavefunction of the two bound electrons, prior to scattering, can be approximated as a product of two single-bound-electron wavefunctions, one centered on each binding structure, $\psi_{1,2} = \phi_1 \phi_2$. Further, scattering is assumed to occur in the non-ionizing (and the elastic) regime, so the spatial wavefunction will take the same form after scattering. The ground state single-bound-electron wavefunctions and energies are calculated by simple diagonalization of the Hamiltonian for a single binding structure.

Thirdly, the tight binding of the bound electrons means that the three-electron wavefunction can be approximated as a product of two single-bound-electron wavefunctions and a single-propagating-electron wavefunction when a propagating electron is in one of the ideal regions far from a binding structure, and as a product of a two-electron wavefunction and a single-bound-electron wavefunction when a propagating electron is in the vicinity of a binding structure.

Fourthly, calculations are restricted to the elastic scattering regime, so only one value of $|k|$ is necessary to describe the propagating electron for each value of the system energy E . However, in the spin subspace $S_z = \frac{1}{2}$, there are three spin states: $|\downarrow\rangle_p |\uparrow\uparrow\rangle$ (I), $|\uparrow\rangle_p |\downarrow\downarrow\rangle$ (II) and $|\uparrow\rangle_p |\uparrow\downarrow\rangle$ (III), where $|\downarrow\rangle_p$ is the state of the propagating electron. For those sections of the wavefunction in which a propagating electron is in one of the ideal regions far from a binding structure, a separate component must be defined for each of the spin states I, II, and III. The usual scattering boundary conditions are used, so there will be three reflection amplitudes (r_{I-III}), three transmission amplitudes (p_{I-III}), and three amplitudes characterizing each of the left-traveling and the right-traveling waves in the intermediate region (A, B_{I-III}). For those sections of the wavefunction in which a propagating electron is in the vicinity of a binding structure (and hence of another electron) the two-electron element of the wavefunction has two components, describing the parallel and antiparallel configurations of the spins. All calculations are carried out in the $S_z = \frac{1}{2}$ subspace, and there are no explicit spin-flip terms, so the spin of the third electron, bound at the other binding structure, follows immediately. For convenience, the position of the flying electron is labeled as n_1 , while the positions of the leftmost and rightmost bound electrons are labeled as n_2 and n_3 respectively. The form of the wavefunction can then be summarized as

$$\Psi(n_1, n_2, n_3) = \begin{pmatrix} \psi_{\downarrow\uparrow}(n_1, n_2) \phi_{\uparrow}(n_3) \\ \psi_{\uparrow\uparrow}(n_1, n_2) \phi_{\downarrow}(n_3) \end{pmatrix}, \quad (5)$$

where $n_1 \approx n_2 \approx x_1, n_3 \approx x_2$,

$$\Psi(n_1, n_2, n_3) = \begin{pmatrix} \psi_{\downarrow\uparrow}(n_1, n_3) \phi_{\uparrow}(n_2) \\ \psi_{\uparrow\uparrow}(n_1, n_3) \phi_{\downarrow}(n_2) \end{pmatrix}, \quad (6)$$

where $n_1 \approx n_3 \approx x_2, n_2 \approx x_1$,

$$\Psi = \begin{pmatrix} (e^{ikn_1} + r_I e^{-ikn_1}) \phi_{\uparrow}(n_2) \phi_{\uparrow}(n_3) \\ r_{II} e^{-ikn_1} \phi_{\downarrow}(n_2) \phi_{\uparrow}(n_3) \\ r_{III} e^{-ikn_1} \phi_{\uparrow}(n_2) \phi_{\downarrow}(n_3) \end{pmatrix}, \quad (7)$$

where $n_1 \ll x_1$ (here the initial spin state is set to I , so the bound electrons are in the state $|\uparrow\uparrow\rangle$), and

$$\Psi = \begin{pmatrix} (A_I e^{ikn_1} + B_I e^{-ikn_1}) \phi_\uparrow(n_2) \phi_\uparrow(n_3) \\ (A_{II} e^{ikn_1} + B_{II} e^{-ikn_1}) \phi_\downarrow(n_2) \phi_\uparrow(n_3) \\ (A_{III} e^{ikn_1} + B_{III} e^{-ikn_1}) \phi_\uparrow(n_2) \phi_\downarrow(n_3) \end{pmatrix}, \quad (8)$$

where $x_1 \ll n_1 \ll x_2$,

$$\Psi = \begin{pmatrix} p_I e^{ikn_1} \phi_\uparrow(n_2) \phi_\uparrow(n_3) \\ p_{II} e^{ikn_1} \phi_\downarrow(n_2) \phi_\uparrow(n_3) \\ p_{III} e^{ikn_1} \phi_\uparrow(n_2) \phi_\downarrow(n_3) \end{pmatrix}, \quad (9)$$

where $x_2 \ll n_1$.

The approximate two-electron state, one-electron state product wavefunctions of the form of equation (5) are connected to the three one-electron state product wavefunctions of the form of equation (7) by boundary conditions of the form

$$[\psi_{\downarrow\uparrow}(n_1, n_2) \phi_\uparrow(n_3)] \rightarrow \begin{cases} \psi_{L1}, & n_1 \ll x_1 \\ \psi_{R1}, & n_1 \gg x_1, \end{cases} \quad (10)$$

(for the case $n_1 \approx n_2 \approx x_1, n_3 \approx x_2$), where

$$\psi_{L1} = \begin{pmatrix} (e^{ikn_1} + r_I e^{-ikn_1}) \phi_\uparrow(n_2) \phi_\uparrow(n_3) \\ r_{II} e^{-ikn_1} \phi_\downarrow(n_2) \phi_\uparrow(n_3) \end{pmatrix}, \quad (11)$$

$$\psi_{R1} = \begin{pmatrix} (A_I e^{ikn_1} + B_I e^{-ikn_1}) \phi_\uparrow(n_2) \phi_\uparrow(n_3) \\ (A_{II} e^{ikn_1} + B_{II} e^{-ikn_1}) \phi_\downarrow(n_2) \phi_\uparrow(n_3) \end{pmatrix}. \quad (12)$$

Scattering is characterized by the reflection and transmission amplitudes r_{I-III} and p_{I-III} , which are obtained by solving the Schrödinger equation as a set of linear equations for the traveling wave amplitudes, and the values of the two-electron wavefunction elements $\psi_{\downarrow\uparrow}(n_1, n_2)$, $\psi_{\uparrow\uparrow}(n_1, n_2)$, $\psi_{\downarrow\uparrow}(n_1, n_3)$ and $\psi_{\uparrow\uparrow}(n_1, n_3)$ on the discretized space in the neighborhood of the respective binding structures. Calculations were carried out at the range of system energies set by two electrons bound in the ground states of the (identical) binding structures, ε_b , and one electron propagating in the ideal leads. This gives $E = 2\varepsilon_b - 2t \cos k$, with k restricted to the range $k \in [0, \pi]$. Transmission probabilities conditional on leaving the bound electrons in a given spin state (calculated as $P_{I-III} = |p_{I-III}|^2$ and referred to as ‘partial transmittivities’, since there are multiple scattering channels) and entanglement data are displayed in this study as functions of the energy of the propagating electron.

In the $S_z = \frac{1}{2}$ subspace, the spin states of the two bound electrons are $|\uparrow\uparrow\rangle$, $|\downarrow\uparrow\rangle$ and $|\uparrow\downarrow\rangle$, corresponding to the three-electron states I, II and III respectively. Entanglement will arise from the simultaneous presence of II and III, which is indicated by the measurement of a transmitted electron in the state $|\uparrow\rangle$. Entanglement can be quantified via concurrence [28, 29], which in the elastic regime of this scattering process can be written in terms of the transmission amplitudes as

$$C = \frac{2 |p_{\uparrow\downarrow} p_{\downarrow\uparrow}|}{|p_{\uparrow\downarrow}|^2 + |p_{\downarrow\uparrow}|^2}, \quad (13)$$

where the denominator is a normalization factor equal to the probability of measuring a transmitted electron in the required

spin-up state. This probability is referred to as the ‘probability of success’, i.e. it is the probability of measuring a transmitted electron as being in the spin state that allows for entanglement (not necessarily full) between the bound electrons.

Before reporting the results obtained from this scheme, it will be useful to briefly revisit a similar scheme explored in previous studies [19–23], in which interactions between propagating and static spins are represented in a point s–d model. In this model, the static spins are handled as a set of external spin states which interact with the spin of the propagating electron via an exchange-type interaction when it reaches a specified point in space. In previous studies, two such static spins have been entangled by placing them in series on a one-dimensional structure and propagating an electron along the structure. For the sake of comparison, we can rewrite the Hamiltonian of the point s–d scheme in the language used in this study. Assuming a discretized one-dimensional conductor which is represented with a Hamiltonian of the same form as \hat{H}_R above (with the sum running from $-\infty$ to $+\infty$), we have a point s–d Hamiltonian:

$$\begin{aligned} \hat{H}_{\text{PSD}} = & \sum_{[n,q]=[x_1,z_1],[x_2,z_2]} \mu_1 [n_{n\uparrow} n_{q\uparrow} + n_{n\downarrow} n_{q\downarrow}] \\ & + [\mu_2 + \lambda c_{n\downarrow}^\dagger c_{q\uparrow}^\dagger c_{n\uparrow} c_{q\downarrow}] n_{n\uparrow} n_{q\downarrow} \\ & + [\mu_2 + \lambda c_{n\uparrow}^\dagger c_{q\downarrow}^\dagger c_{n\downarrow} c_{q\uparrow}] n_{n\downarrow} n_{q\uparrow}. \end{aligned} \quad (14)$$

Here, x_1 and x_2 are the points on the 1D conductor of closest approach to the external spins, while z_1 and z_2 are the notional sites, external to the 1D chain, at which the external spins are bound. The interaction parameters are the potential between parallel spins μ_1 , the potential between antiparallel spins μ_2 , and the spin-flip coupling strength λ between antiparallel spins. The most widely used version of this model is based on the dot product of the two spins and an exchange parameter J , and hence has the relations $\lambda = -2\mu_2 = 2\mu_1$.

For reference, the transmission spectra are calculated with these relations for an electron scattering from two point s–d spins in series, using the analog of the method outlined above. Exchange coupling strength is $\lambda = t$, and there are three intermediate sites. The starting state is $|\downarrow\rangle_p |\uparrow\uparrow\rangle$. The transmission probabilities for each of the spin states in the $S_z = \frac{1}{2}$ subspace are plotted in figure 2(a), labeled in terms of the spins of the two static spins. Transmission into the (unentangled) $|\uparrow\uparrow\rangle$ state of the static spins generally predominates, however there is a significant chance of scattering into one of the two individually unentangled, simple antiparallel spin states that are necessary for entanglement. Most important is that these probabilities be both equal and as high as possible at the same energy. This means that entanglement will be close to full ($C \sim 1$) if the propagating electron is measured as being transmitted and in the correct spin state ($|\uparrow\rangle$), and that there is a high probability of this favorable measurement being made. Addressing these criteria, both the concurrence (calculated from the transmission amplitudes using equation (14)) and the chance of achieving a favorable outcome resulting in that concurrence (defined as $P_{II} + P_{III}$) are plotted in figure 2. The result is that full entanglement can indeed be achieved with the correct

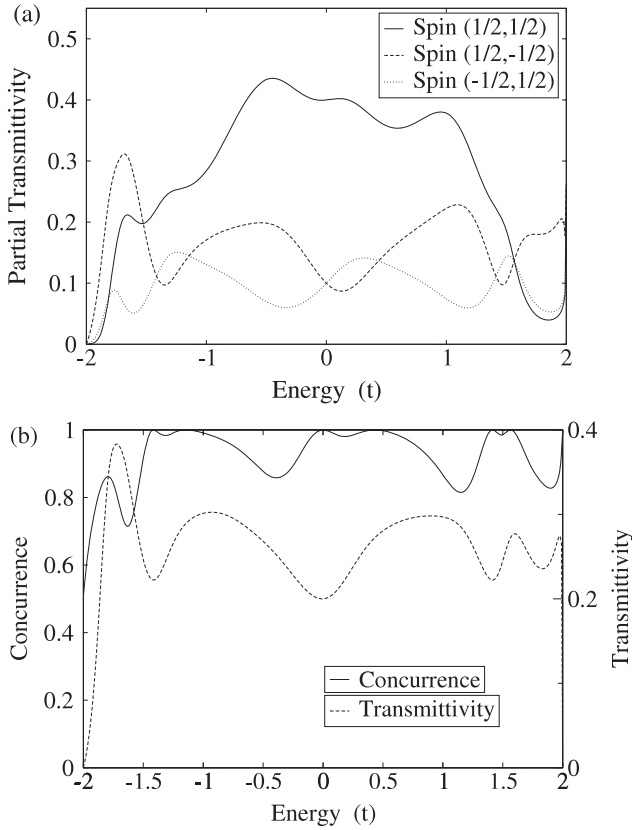


Figure 2. (a) Transmission probabilities for the static spin configurations $(\frac{1}{2}, \frac{1}{2}), (\frac{1}{2}, -\frac{1}{2})$ and $(-\frac{1}{2}, \frac{1}{2})$ from the starting state $(\frac{1}{2}, \frac{1}{2})$. (b) Concurrence and probability of success for an entangled state, $P_{II} + P_{III}$. Parameters used $\lambda = t, \mu_1 = t/2, \mu_2 = -t/2, 3$ intermediate sites. See section 2, equations (5)–(12), equation (13) and accompanying discussion for more details.

propagation energy, and that a favorable result to the scattering process will be achieved with a low but still significant probability: often >0.2 , and reaching a maximum value of 0.3.

The generation of entanglement with a significant probability of success in this system is markedly at odds with the case of electrons at two single-state binding structures in series [17], in which full entanglement does not occur with any significant probability of success. The reason for this difference is the Pauli exclusion effect in the single-state binding structure, which results in strong singlet filtering [13]. The use of two-state binding structures in this study is an attempt to overcome this effect in a specifically quantum-dot-based system. In fact, the ‘stub’ structure studied here maps on to the point s–d model, in the regime $\mu_2 = -\lambda, \lambda < 1, \mu_1 \ll 1$ (point s–d model), which is equivalent to $|\varepsilon_0| \gg t$ and $U \geq 2\varepsilon_0$ (real-space Anderson ‘stub’ structure). A minor variation of Hewson’s derivation [14] of the s–d model from the Anderson model gives the interaction parameters

$$\lambda = t_c^2 \left[\frac{1}{\varepsilon_0 + U} - \frac{1}{\varepsilon_0} \right], \quad (15)$$

$$\mu_1 \approx -\frac{t_c^2}{\varepsilon_0}. \quad (16)$$

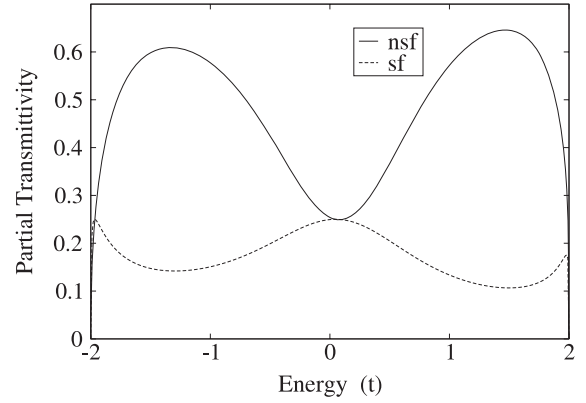


Figure 3. Non-spin-flip and spin-flip transmission probabilities for a single stub structure with one bound electron. Parameters used $\varepsilon_0 = -10t, U = -\varepsilon_0$, and $t' = t = t_c$.

3. The stub structure

The ‘stub’ two-state binding structure consists of a one-state quantum dot placed to one side of a one-dimensional wire, and coupled to the adjacent segment; this segment is the spatially-defined second ‘state’ (the site to which the quantum dot is coupled, in the discrete model used in this study). In the general representation of a two-state binding structure shown in figure 1, this corresponds to $\varepsilon_\alpha = U_\alpha = 0, \varepsilon_\beta = \varepsilon_0, U_\beta = U, V = 0, t_1 = t', t_2 = 0$. The calculations in this study are carried out in the non-ionizing regime, so $\varepsilon_0 \ll -t$. Scattering calculations are carried out over the energy band for an electron bound at each structure and a propagating electron, that is $2\varepsilon_b - 2t < E < 2\varepsilon_b + 2t$ (corresponding to $k \in [0, \pi]$). For this structure, in the non-ionizing regime, the ground state single-electron bound state energy is $\varepsilon_b \approx \varepsilon_0 + \frac{t_c^2}{\varepsilon_0}$, and the first excited state energy is $\varepsilon_{xs} \approx -\frac{t_c^2}{\varepsilon_0}$, so the elastic regime extends across the entire band. Finally, in order to produce entanglement between the two bound electrons, a significant amplitude for spin-flip scattering (that is, the transmitted or reflected electron being a different spin to the incident electron, indicating a swap in the electron occupying the binding structure) is desirable. To achieve this, a resonance with the energy of the two-electron occupancy state will produce a resonant peak in the spin-flip scattering amplitudes. Such a resonance will occur for some energy in the band if $-2t < \varepsilon_0 + U < 2t$.

To help clarify the spin-dependent scattering behavior of an electron from two electrons bound at stub structures in series, the spin-dependent scattering behavior of an electron from a single bound electron at a stub structure is presented in figure 3. Within the constraints of the stub structure, the parameters used are $\varepsilon_0 = -10t, U = -\varepsilon_0$, and $t' = t = t_c$. The transmission probabilities are shown for non-spin-flip and spin-flip scattering. By symmetry, the reflection probabilities are equal to the spin-flip transmission probability, except at the very top and bottom of the band.

In the limit $\varepsilon_0 \rightarrow -\infty$, the transmission amplitudes can be shown through straightforward but tedious algebra to be

$$p_{\text{nsf}} = \frac{t_c^2 + 2it \sin k (2t \cos k - (\varepsilon_0 + U))}{2t_c^2 + 2it \sin k (2t \cos k - (\varepsilon_0 + U))}, \quad (17)$$

$$p_{\text{sf}} = \frac{-t_c^2}{2t_c^2 + 2it \sin k (2t \cos k - (\varepsilon_0 + U))}, \quad (18)$$

and in this limit $r_{\text{nsf}} = r_{\text{sf}} = p_{\text{sf}}$. These formula accurately describe the scattering for finite ε_0 except at the very top and bottom of the band. Examination of these formulae or figure 3 shows that when $-2t \cos k = \varepsilon_0 + U$ a resonance will occur at which $P_{\text{nsf}} = P_{\text{sf}} = R_{\text{nsf}} = R_{\text{sf}} = 0.25$, a peak in the probability of spin-flip scattering (and a minimum in the probability of non-spin-flip scattering).

In figure 4(a), the scattering probabilities to bound electron spin states $|\uparrow\uparrow\rangle$, $|\uparrow\downarrow\rangle$ and $|\downarrow\uparrow\rangle$ from the starting state $|\downarrow\rangle_p|\uparrow\uparrow\rangle$ are presented for an electron scattering from two electrons bound at stub structures in series. The parameters used are once again $\varepsilon_0 = -10t$, $U = -\varepsilon_0$, and $t' = t = t_c$, with 3 intermediate sites. Again, the simultaneous presence of states $|\uparrow\downarrow\rangle$ and $|\downarrow\uparrow\rangle$ will give entanglement. Transmission probabilities that are near-equal will yield a highly entangled state of the bound electrons if a transmitted electron is measured to be spin-up. High transmission probabilities for these states indicates a higher probability of obtaining this successful outcome. Figure 4(b) plots the concurrence achieved across the propagating electron band along with the probability of obtaining the corresponding successful outcome to the scattering process ($P_{\text{II}} + P_{\text{III}}$).

Probability of success is low but still significant (typically > 0.15) at energies that allow for full entanglement, with a maximum probability of success at full entanglement of ~ 0.23 . These figures are comparable to those found with the point s-d model. However, in the regime used here to obtain these probabilities, the stub structure does not map on to the point s-d model, since obtaining a reasonably high spin-flip amplitude at individual stub structures approximately requires $-2t < \varepsilon_0 + U < 2t$, that is $\varepsilon_0 \sim -U$, whereas correspondence with a point s-d scenario requires $U \geq -2\varepsilon_0$.

4. Two quantum dot structure

The ‘double quantum dot’ structure consists of one binding state embedded in a one-dimensional wire, and coupled to a second binding state to the side of the wire. In the general representation of a two-state binding structure shown in figure 1, this corresponds to $\varepsilon_\alpha = \varepsilon_\beta = \varepsilon_0$ and $U_\alpha = U_\beta = U$. We also set $t_2 = 0$. The non-ionizing regime is again defined by $\varepsilon_0 \ll -t$. In this structure, the ground state single-electron bound state energy is $\varepsilon_b \approx \varepsilon_0 - t_c$, and the first excited state energy is given by $\varepsilon_{xs} \approx \varepsilon_0 + t_c$. The coupling strength t_c is set at a physically realistic maximum of t . The elastic regime of the energy band for two bound electrons at two binding structures and one propagating electron is therefore $2\varepsilon_b - 2t < E < 2\varepsilon_b$, corresponding to $k \in [0, \frac{\pi}{2}]$. Scattering behavior is calculated in this range. For this structure, the introduction of a strongly binding and strongly backscattering state in the main line of the one-dimensional wire means that a strong Coulomb repulsion, U , is necessary to allow a high probability for transmission, hence it is required that $-2t < \varepsilon_0 + U < 0$. To avoid the kind of spin-filtering created by a single-state binding structure, it is also necessary to have a

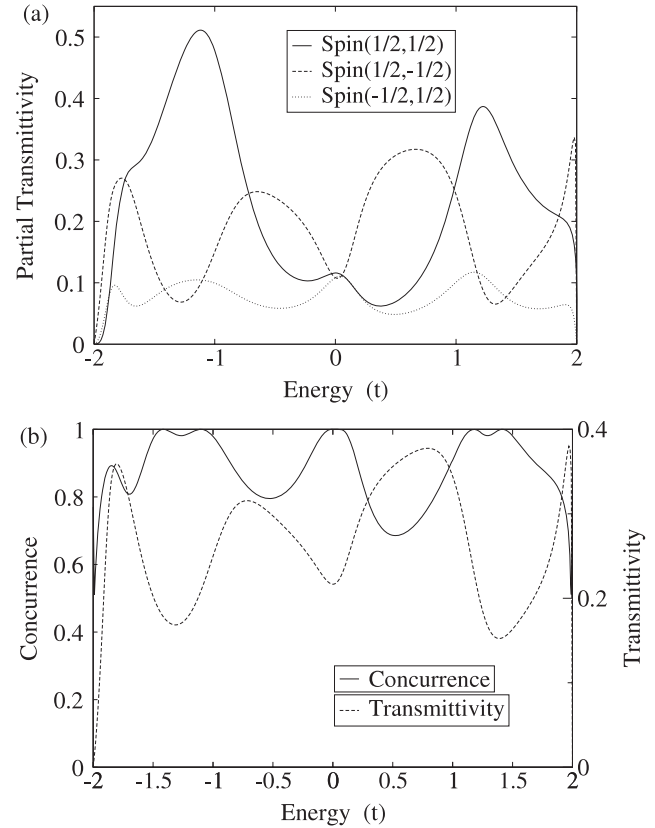


Figure 4. (a) Transmission probabilities for the bound electron spin configurations $(\frac{1}{2}, \frac{1}{2})$, $(\frac{1}{2}, -\frac{1}{2})$ and $(-\frac{1}{2}, \frac{1}{2})$ in stub structures from the starting state $(\frac{1}{2}, \frac{1}{2})$. (b) Concurrence and probability of success for an entangled state, $P_{\text{II}} + P_{\text{III}}$. Parameters used $\varepsilon_0 = -10t$, $U = -\varepsilon_0$, and $t' = t = t_c$. 3 intermediate sites. See section 2, equations (5)–(12), equation (13) and accompanying discussion for more details.

high probability of transmission for the triplet configuration of the bound and propagating electrons, so the interstate Coulomb repulsion V must also be sufficiently high: $-2t < \varepsilon_0 + V < 0$.

Once again, the spin-dependent scattering behavior of a single binding structure is presented in order to illuminate the behavior of two binding structures in series. The behavior of one-electron scattering from another bound at a two quantum dot structure is plotted in figure 5. Within the constraints of the two quantum dot structure, the parameters used are $\varepsilon_0 = -10t$, $U = -\varepsilon_0 - t$, $V = 0.95U$ and $t' = t = t_c$. The transmission probabilities are shown for non-spin-flip and spin-flip scattering. The transmission characteristics of this kind of structure have been discussed elsewhere by the authors of this study [13]. Briefly, they can be explained by noting that the two-electron wavefunction in the vicinity of the binding structure during scattering can be approximated as a sum of four eigenstates with energies close to those of the system being examined, and hence four peaks are expected in the transmission spectrum. As expected, there are two peaks in the non-spin-flip spectrum and two peaks in the spin-flip spectrum.

In figure 6(a), the scattering probabilities to bound electron spin states $|\uparrow\uparrow\rangle$, $|\uparrow\downarrow\rangle$ and $|\downarrow\uparrow\rangle$ from the starting state $|\downarrow\rangle_p|\uparrow\uparrow\rangle$ are presented for an electron scattering from two

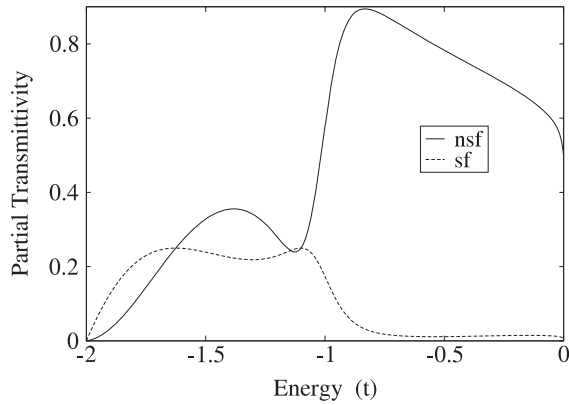


Figure 5. Non-spin-flip and spin-flip transmission probabilities for a single two quantum dot structure with one bound electron. Parameters used $\varepsilon_0 = -10t$, $U = -\varepsilon_0 - t$, $V = 0.95U$, and $t' = t = t_c$.

electrons bound at two quantum dot structures in series. The parameters used are $\varepsilon_0 = -10t$, $U = -(\varepsilon_0 + t)$, $V = 0.95U$ and $t' = t = t_c$, with 3 intermediate sites. Figure 6(b) plots the concurrence achieved across the propagating electron band along with the probability of obtaining the corresponding successful outcome to the scattering process ($P_{II} + P_{III}$).

Full entanglement is achieved in two narrow regions of the propagating energy band and the elastic scattering regime. At both these points, the probability of containing the required outcome to the scattering process is significant, ranging from ~ 0.17 to a maximum of ~ 0.24 . These figures are slightly higher than those for the stub binding structure, although of course any implementation of this double quantum dot binding structure will be complicated relative to the stub structure by the increased possibility of inelastic scattering, and the necessity of a relatively high interstate Coulomb repulsion.

The two quantum dot binding structure will not map on to the point s-d model in any parameter regime of interest to the generation of entanglement, since the requirement that $U \sim V$ means that states in which two electrons of opposite spin occupy the same spatial state will be as important as states in which one electron occupies each spatial state. Mapping to the point s-d model excludes such states, except as ‘virtual’ excitations.

5. Summary and conclusions

Two-state binding structures based on the ‘real-space Anderson model’ represent a quasi-zero-dimensional structure within, for example, a carbon nanotube or quantum wire, such as a gate-defined quantum dot with multiple accessible electronic states. They can be used to bind an electron so its spin can be used as a qubit. In this study, the scattering behavior has been calculated in the elastic regime and the $S_z = \frac{1}{2}$ spin subspace for one propagating electron scattering from two electrons bound in series at separate binding structures in a one-dimensional wire. In particular, it has been shown that for the correct energy (and hence wavevector) of the propagating electron, spin-flip scattering events can result in a fully entangled state of the

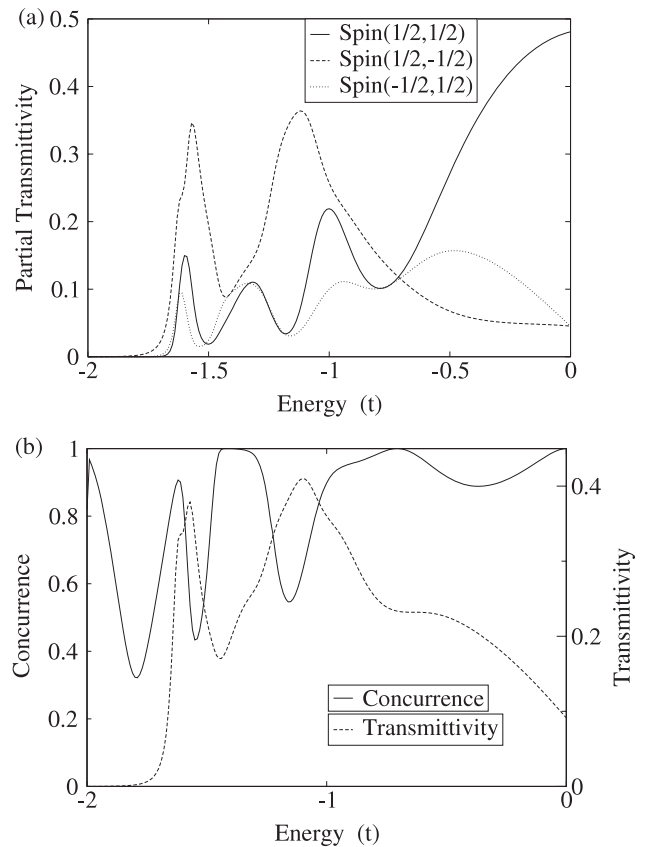


Figure 6. (a) Transmission probabilities for the bound electron spin configurations $(\frac{1}{2}, \frac{1}{2})$, $(\frac{1}{2}, -\frac{1}{2})$ and $(-\frac{1}{2}, \frac{1}{2})$ in two quantum dot structures from the starting state $(\frac{1}{2}, \frac{1}{2})$. (b) Concurrence and probability of success for an entangled state, $P_{II} + P_{III}$. Parameters used $\varepsilon_0 = -10t$, $V = 0.95U$, $U = -\varepsilon_0 - t$, and $t' = t = t_c$. 3 intermediate sites. See section 2, equations (5)–(12), equation (13) and accompanying discussion for more details.

two bound electrons. Obtaining such a fully entangled state is dependent upon measurement of a transmitted, propagating electron with spin state $|\uparrow\rangle_p$.

The entanglement (quantified as concurrence) spectrum and probability of obtaining a favorable outcome to the scattering process as a function of propagation energy have been calculated, along with the basic scattering amplitudes for the three possible spin states, for two types of two-state binding structure. One of these was a ‘stub’ structure, in which a single-state binding site is coupled to one segment of the 1D wire, with the segment acting as a second ‘state’. In this case full entanglement was obtained with a maximum probability of success of ~ 0.23 . The other was a ‘double-quantum-dot’ structure, with one binding state embedded in the 1D wire and a second coupled to it from the side. Full entanglement was achieved with a maximum probability of success of ~ 0.24 . Although this is slightly higher than the stub structure, it should be noted that implementations of the double-quantum-dot structure will be complicated by the possibility of inelastic scattering (especially at low values of interstate coupling, t_c) and the necessity for a high interstate Coulomb repulsion (V). We have obtained analogous results for the ‘point s-d’ model, as applied in the discretized one-dimensional structure used in this study.

The ability to produce entanglement between two electrons bound in series at two-state binding structures, by scattering a third electron from them, is a considerable improvement on the situation for single-state binding structures [17]. In the latter case, entanglement is only generated with a very low probability of success ($\sim 10^{-4}$). The reason for this difference is that the combination of backscattering and Coulomb-mediated resonance in the single-state structures leads to very strong singlet/triplet filtering in the spin states of the propagating electron and each bound electron; information about previous scattering events is therefore almost completely erased each time the propagating electron scatters from a bound electron of the opposite spin. The use of two (energetically accessible) states at each binding structure eliminates this effect. This is in distinction the approach taken in the authors' previous work [17], in which a symmetric parallel configuration was used to obtain simultaneous interactions with both bound electrons.

While the probability of success in generating entanglement with a pair of two-state binding structures is not high, it is certainly significant; and it should be noted that the parameters used here were not rigorously optimized with respect to probability of success. Some improvement from the figures reported here is therefore expected with careful tuning of the systems involved. Additionally, recent results [30] suggest that repeated scattering of propagating electrons from bound spins may give rise to a sequence of states that converges on full entanglement, even though each individual step is only partially entangling.

Given the ever-increasing degree of control that is experimentally available over single electrons in quantum dots, the authors hope that these results can act as a guide to workers in solid state quantum computation in the not-too-distant-future.

Acknowledgments

This work is a part of QIP IRC; MH is supported by an EPSRC DTA; GADB is supported by an EPSRC Professional Research Fellowship; JHJ acknowledges support from the UK Ministry of Defense. The authors would like to thank Professor D G Pettifor for useful discussions.

References

- [1] Austing D G, Honda T, Muraki K, Tokura Y and Tarucha S 1998 *Physica B* **249–251** 206
- [2] Hanson R, Kouwenhoven L P, Petta J R, Tarucha S and Vandersypen L M K 2007 *Rev. Mod. Phys.* **79** 1217
- [3] van der Wiel W G, Stopa M, Koderer T, Hatano T and Tarucha S 2006 *New J. Phys.* **8** 28
- [4] Nowack K C, Koppens F H L, Nazarov Y V and Vandersypen L M K 2007 *Science* **318** 1430
- [5] Amasha S, Maclean K, Radu I P, Zumbuhl D M, Kastner M A, Hanson M P and Gossard A C 2008 *Phys. Rev. Lett.* **100** 046803
- [6] Benjamin S C, Ardavan A, Briggs G A D, Britz D A, Gunlycke D, Jefferson J H, Jones M A G, Leigh D F, Lovett B W, Khlobystov A N, Lyon S A, Morton J J L, Porfyrakis K, Sambrook M R and Tyryshkin A M 2006 *J. Phys.: Condens. Matter* **18** S867
- [7] Ardavan A, Austwick M, Benjamin S C, Briggs G A D, Dennis T J S, Ferguson A, Hasko D G, Kanai M, Khlobystov A N, Lovett B W, Morley G W, Oliver R A, Pettifor D G, Porfyrakis K, Reina J H, Rice J H, Smith J D, Taylor R A, Williams D G, Adelman C, Mariette H and Hamers R J 2003 *Phil. Trans. R. Soc. A* **361** 1473
- [8] Saito R, Dresselhaus G and Dresselhaus M S 1998 *Physical Properties of Carbon Nanotubes* (London: Imperial College Press)
- [9] Tsukagoshi K, Alphenaar B W and Ago H 1999 *Nature* **401** 572
- [10] Biercuk M J, Garaj S, Mason N, Chow J M and Marcus C M 2005 *Nano Lett.* **5** 1267
- [11] Jorgensen H I, Grove-Rasmussen K, Hauptmann J R and Lindelhof P E 2006 *App. Phys. Lett.* **89** 232113
- [12] Graber M R, Coish W A, Hoffmann C, Weiss M, Furer J, Oberholzer S, Loss D and Schönenberger C 2006 *Phys. Rev. B* **74** 075427
- [13] Habgood M, Jefferson J H, Ramšak A, Pettifor D G and Briggs G A D 2008 *Phys. Rev. B* **77** 075337
- [14] Hewson A 1993 *The Kondo Problem to Heavy Fermions* (Cambridge: Cambridge University Press)
- [15] Jefferson J H, Ramšak A and Rejec T 2006 *Europhys. Lett.* **74** 764
- [16] Gunlycke D, Jefferson J H, Rejec T, Ramšak A, Pettifor D G and Briggs G A D 2006 *J. Phys.: Condens. Matter* **18** S851
- [17] Habgood M, Jefferson J H and Briggs G A D 2008 *Phys. Rev. B* **77** 195308
- [18] Coffman V, Kundu J and Wootters W K 2000 *Phys. Rev. A* **61** 052306
- [19] Costa A T Jr, Bose S and Omar Y 2006 *Phys. Rev. Lett.* **96** 230501
- [20] Ciccarello F, Palma G M, Zarcone M, Omar Y and Vieira V R 2006 *New J. Phys.* **8** 214
- [21] Ciccarello F, Palma G M, Zarcone M, Omar Y and Vieira V R 2007 *J. Phys. A: Math. Theor.* **40** 7993
- [22] Ciccarello F, Palma G M, Zarcone M, Omar Y and Vieira V R 2007 *Laser Phys.* **17** 889
- [23] Yuasa K and Nakazato H 2007 *J. Phys. A: Math. Theor.* **40** 297
- [24] Browne D E and Plenio M B 2003 *Phys. Rev. A* **67** 012325
- [25] Leuenberger M N, Flatte M E and Awschalom D D 2005 *Phys. Rev. Lett.* **94** 107401
- [26] Kroutvar M, Ducommun Y, Heiss D, Bichler M, Scuh D, Abstreiter D and Finley J J 2004 *Nature* **432** 81
- [27] Loss D and Sukhorukov E V 2000 *Phys. Rev. Lett.* **84** 1035
- [28] Wootters W K 1998 *Phys. Rev. Lett.* **80** 2245
- [29] Ramšak A, Sega I and Jefferson J H 2006 *Phys. Rev. A* **74** 010304
- [30] Ciccarello F, Paternostro M, Kim M S and Palma G M 2008 *Phys. Rev. Lett.* **100** 150501